Supplementary Material

High-purity Capture and Release of Circulating Exosomes using an Exosome-specific Dual-patterned Immunofiltration (ExoDIF) Device

Yoon-Tae Kang[1, †], Young Jun Kim[1, †], Jiyoon Bu[1], Young-Ho Cho[1, *], Sae Won Han[2], and Byung-In Moon[3]

[1]Cell Bench Research Center, Korea Advanced Institute of Science and Technology (KAIST),

291 Daehak-ro, Yuseong-gu, Daejeon 34141, Republic of Korea

E-mail: nanosys@kaist.ac.kr

[2]Colorectal Cancer Center, Seoul National University Cancer Hospital,

101, Daehak-ro, Jongno-gu, Seoul 03080, Republic of Korea

[3]College of Medicine, Ewha Womans University and Ewha Medical Research Institute, 911-1,

MokDong, YangCheon-Ku, Seoul, 07985, Republic of Korea

†Both authors contributed equally to this work

Contents

Figures

Tables

S1. An Overview of the Overall Process

The verification of the Exosome-specific Dual-patterned Immunofiltration (ExoDIF) devices was proceeded as follows.

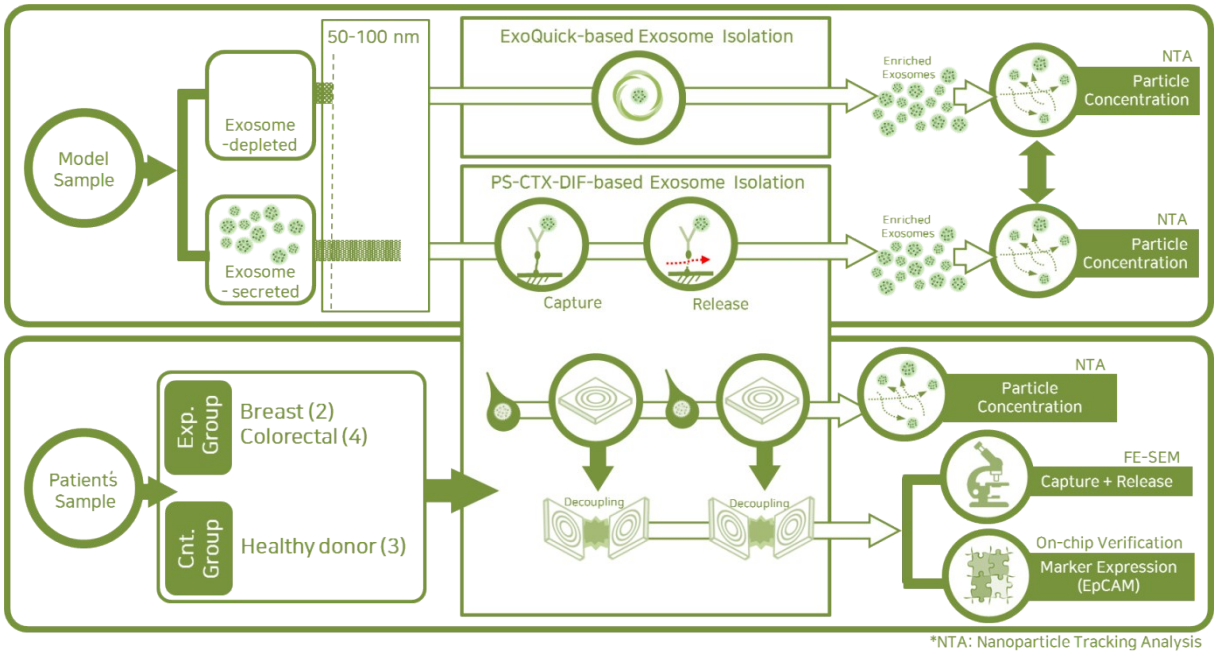

Fig. S1. An overview of the overall experiment using ExoDIF devices

The particle concentration (particles/mL) and proportion (%) were analyzed by nanoparticle tracking analysis. The results were also compared to those of ExoQuick-based exosome isolation. In order to extend our study to clinical use, patients' samples (from 2 breast cancer patients and 4 colorectal cancer patients) and 3 control samples (from healthy donors) was processed by ExoDIF at an aforementioned condition. The performance was evaluated on the basis of capture efficiency, background subtraction efficiency, separation factor, and exosome enrichment ratio. In the meantime, the ability of capture and release was also verified using FE-SEM analysis. The expression of cancer-associated marker on exosome was additionally examined by on-chip fluorescence verification.

S2. Fabrication and Modification Procedure of ExoDIF Device

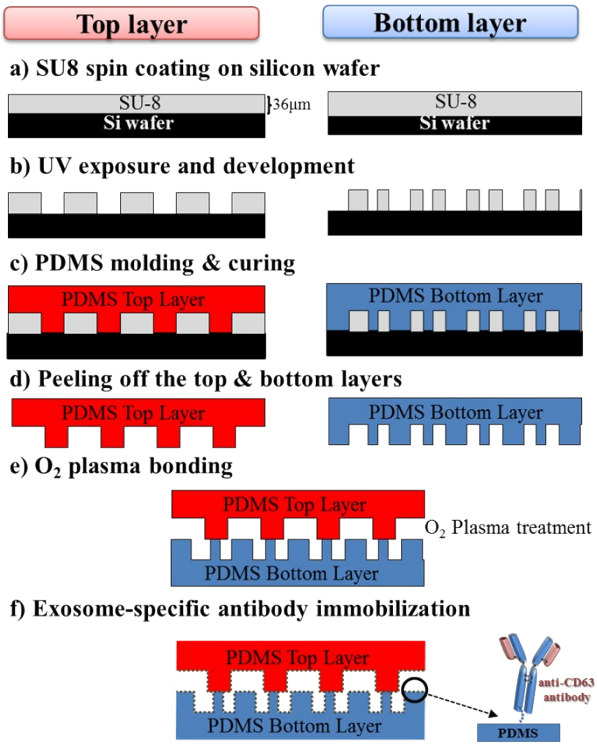

Fig. S2. Fabrication and modification procedure of the ExoDIF device

The mold for the present device was fabricated by patterning SU8-2050 photoresist on a silicon wafer (a). The patterns were oppositely duplicated to the polydimethylsiloxane (PDMS) blocks by conventional micro-molding process (c) followed by curing process (d). As a result, the top and bottom layers were fabricated. The accurate bonding between the layers were done after O_2 plasma treatment (e) with precisely aligning them above the microscope. Then, the immobilization of anti-CD63 antibody in the device was achieved following the crosslinking chemistry and avidin-biotin chemistry (f).

S3. Comparison with the Previous DIF devices

The DIF devices was first presented in 2016 by our group, as a tool for negative selection of heterogeneous circulating tumor cells.[1] At that time, the DIF device was modified with anti-CD45 antibodies for capturing leukocytes; there was no need to recover them because all we needed to collect by using DIF was unreacted circulating tumor cells. In this study, however, DIF was modified to capture circulating exosomes, and it is also nessesary to recover the captured ones at the subsequent stage. Although previous DIF device and ExoDIF devices have identical structure, the surface and antibody-immobilized layer was differently modified with anti-CD63 antibodies via clevabel linkers. Fig. S3 indicates the difference in molecular structure between previous DIF device and ExoDIF devices.

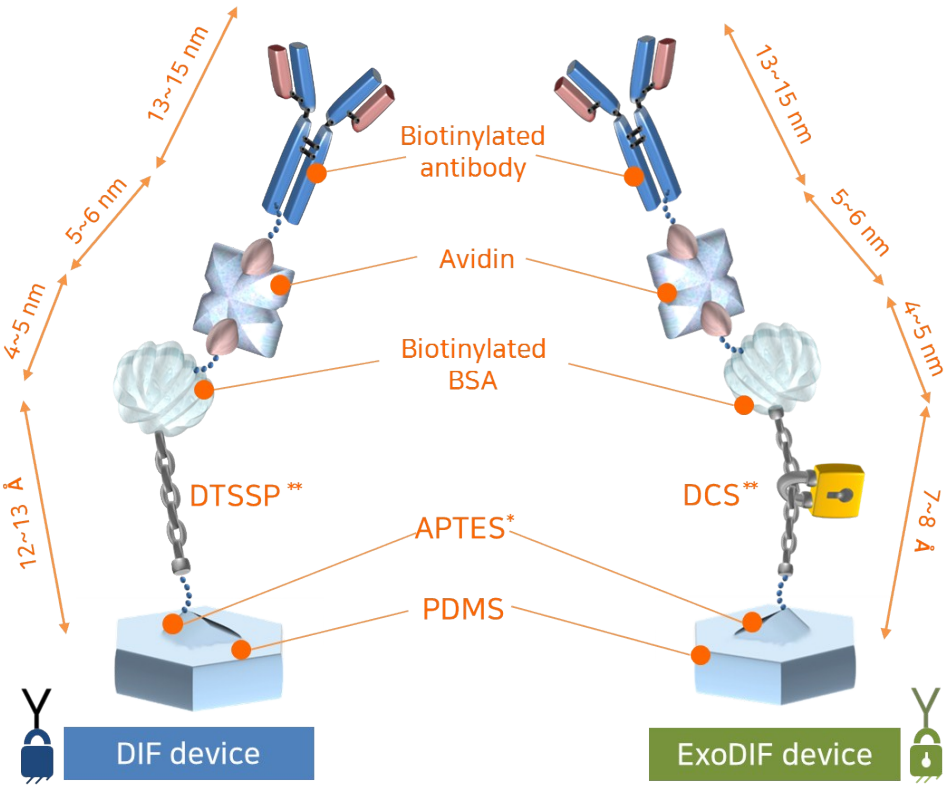

Fig.S3. The molecular design of the layers for DIF and ExoDIF device. In case of DIF device, the cleavable-linker was chosen for the retrieval process (DSC: disuccinimidyl carbonate; DTSSP: Dithiobis(sulfosuccinimidylpropionate)).

Because both previous DIF device and ExoDIF devices are commonly depend on the immunoaffinity- based reaction, we anticipated that the reaction of anti-CD63 antibody-immobilized layer againt exosome also can be enhanced by the help of the structual advantages of DIP devices. The only concern was the differences in size of the target because the diameter of leukocytes is about 100~200 times longer than that of exosomes. However, according to our experience, the differences did not seem to be a significant matter for the following reasons.

(a) The major advantage of DIF device was fluid whirling for the enhancement of reaction between antigen-expressed particles in fluids and antibody-immobilized layers on the surface. The benefit of turbulent micro-mixing is the same for smaller particles as well. As it can be seen in Fig. 5a and 5b, more exosome-sized particles were reacted on the edge of the embossed or engraved patterns. These results indicate that the possibility of reaction was predominantly enhanced due to fluidic whirling.

(b) In the demonstration of previous DIF device, we confirmed the device can contain 16.7 ± 1.5 million of leukocyte; assuming other conditions being equal, the present device can handle at least 10^9 order of exosome-sized particles. Fig. S4 also support our estimation. Although we first considered the applicability to cell filtration when designing DIF device, the expanded surface area of the present device may be more useful in the filtration of particles much smaller than cells.

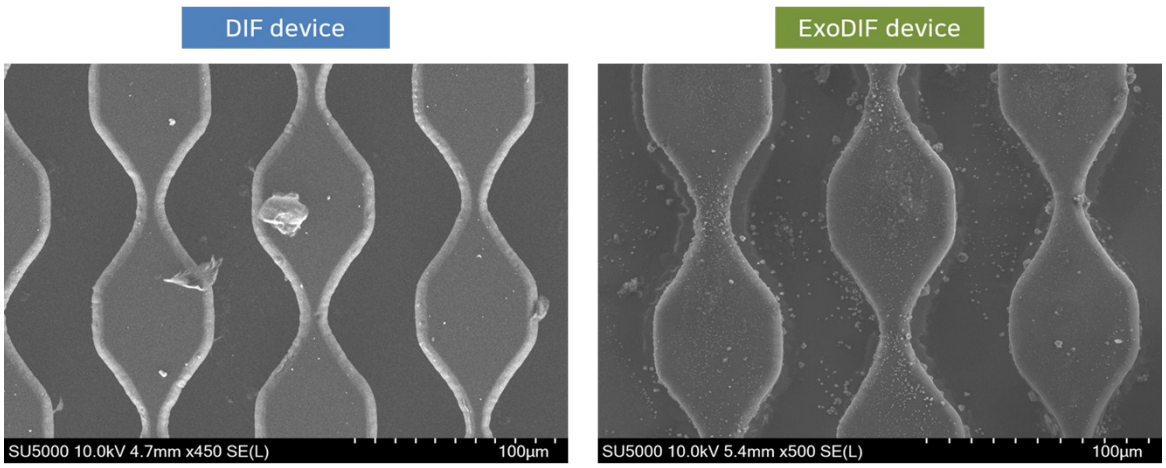

(a) **(b)**

Fig.S4. The patters of DIF and ExoDIF devices after immunofiltaration: (a) the adsorbed cells on the DIF device; (b) the captured exosomes on the ExoDIF device.

S4. A Particle Traveling inside the DIF devices

We designed the DIF device, which is composed of two distinct layers with unique patterns, for archieving a high particle-to-chip collision rate; the bottom layer consisting of evenly spaced octagonal rings that continuously shrinks and expands along the structure and the top layer having engraved rectangular patterns with the regular intervals, which are perpendicular to the octagonal rings on the bottom layer, thus forming bridges between the neighboring rings. The sample was engaged into the central inlet port and spread in a radial direction to eight outlet ports. In Fig. S5a, we utilized yellow ink to the present device for showing how the fluid flows. Additionally, the particles repetatively moved upward and downward during their traveling due to the uniquely engraved patterns. As we described in the manuscript, the total area of the fabricated device was 40 mm × 40 mm, which is large enough to contain approximately 150 octagonal ring patterns. The height of the octagonal rings were designed to be 36 μm, and the longest and the shortest width of the ring structures were 60 μm and 10 μm, respectively and the distance between each ring was 82 μm. The shrinkage and the expansion of the ring was repeated for every 120 μm. the patterns on the top layer was also engraved in 36 μm and the bridge were designed in rectangular shapes having dimension of 36 μm × 132 μm, to minimize the undesired binding. Each of the rectangular bridge was placed above the expanded part of the octagonal rings. Therefore, the particles traveled a longer pathway by the help of fluidic whirling, and the binding chance between the particles and antibody-immobilized patterns also increased appreciably, compared to the conventional devices. Fig. S5b and S5c show the schematic diagram of particle traveling inside the DIF device, with top view and perspective projection view.

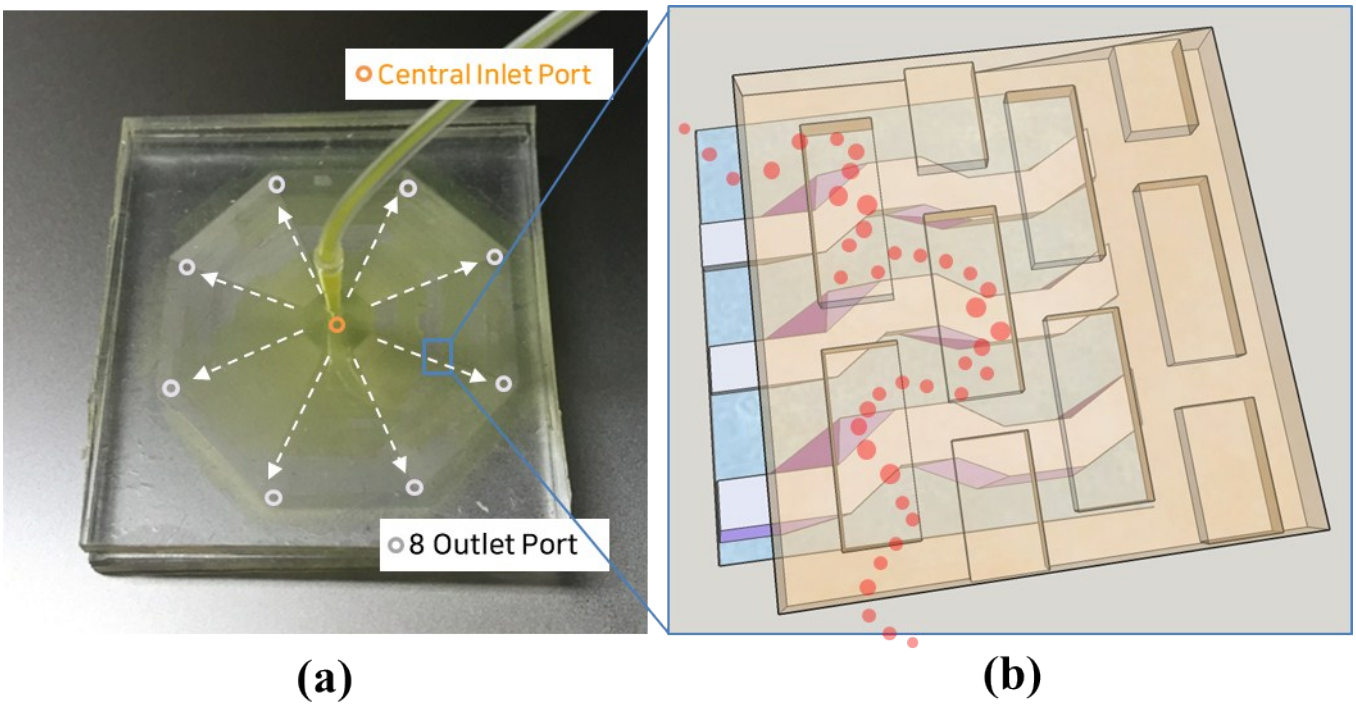

Fig. S5. A Particle traveling inside the DIF devices: (a) spreading of yellow ink in a radial direction; (b) schematic diagram of the particle traveling (top view); (c) schematic diagram of the traveling path (perspective projection view). The red dot indicates the movement of the engaged particles.

S5. Evaluation Criteria for the ExoDIF devices

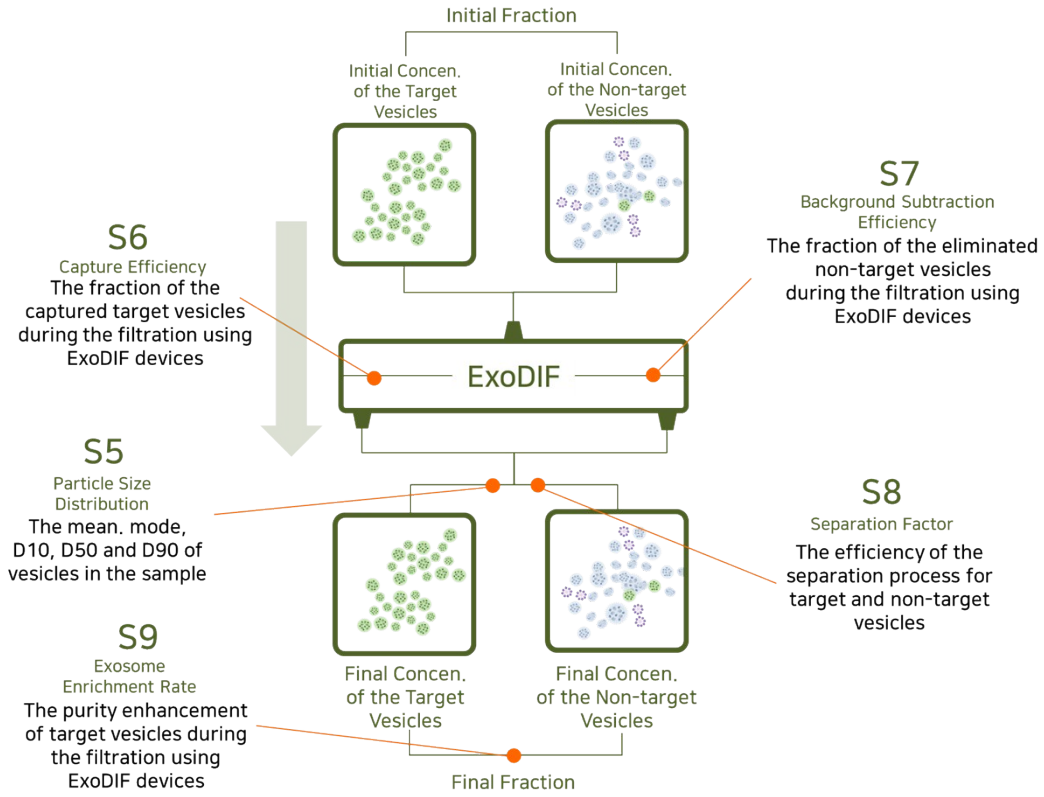

Fig. S6. Evaluation criteria for performance of the ExoDIF devices.

To date, a number of articles have reported microfluidics-based exosome isolation. When they utilized nanoparticle tracking analysis, the particle concentration, proportion, and distribution were usually presented for the calcuration of capture efficiency. In this study, our group tried to consider other factors for the evalation of ExoDIF devices. As a tool for enriching exosome samples with high purity, the ellimination of background vesicles (non-target vesicles) is as important as capture efficicy of exosome-sixed vesicles (target vesicles). Therefore, we present background subtraction efficiency (Section S7), separation factor (Section S8), and exosome enrichment rate (Section S9), along with capture efficiency (Section S6). Each criteria will be discussed in the section designated above.

S6. Size Gating for Exosomes and Other Extracellular Vesicles

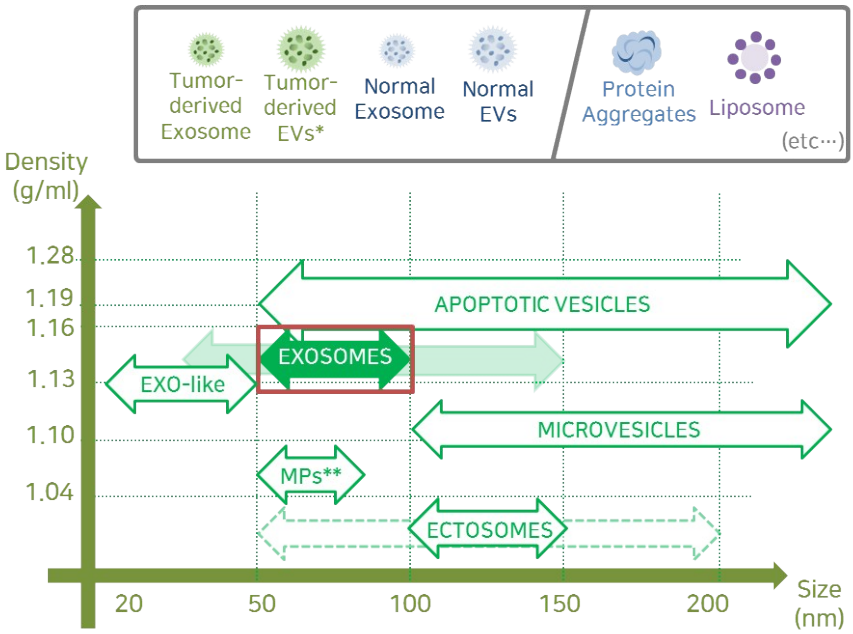

Fig. S7. Variation in size and density of exosome and other extracellular vesicles.

In this experiment, the size gating of the exosome-sized vesicle was critical factor of performance evaluation because the samples are mainly analyzed by means of nanoparticle tracking analysis. Recent studies have proposed different standard in the size gating of exosome: from narrowest (50 ~ 100 nm)[2-4] to widest (30 ~ 200 nm).[5, 6] We followed the narrowest one for two reasons. First, many researchers have pointed out there are diverse contents in the reported range: protein aggregates, liposome, exosome-like vesicles (20~50 nm),[7] membrane particle (50 ~ 80 nm),[8] ectosome (100 ~ 150 nm),[9] apoptotic vesicles (50 ~ 1,000 nm), microvesicles (100 nm ~ 1,000 nm), and so on. Moreover their density range is also overwrapped one another: membrane particle (1.04 ~ 1.07 g/ml), exosome-like vesicles (1.1 g/ml), apoptotic vesicles (1.16 ~ 1.28 g/ml), and exosome (1.13 ~ 1.19 g/ml). That is the reason why most exosome isolation methods often fail to distinguish between differently sized EVs and membrane-free macromolecular aggregates. When considering the principle of

nanoparticle tracking analysis, it is impossible to discriminate exosomes from other particles, with a range above 100 nm. Second, there are differences in mechanism between the present device and ExoQuick kit. Because ExoQuick kit is based on size-dependent precipitates, its performance is more sensitive to the size gating. On the other hand, the present device, which is based on affinity-dependent reaction, captures CD63-expressed particles regardless of size.

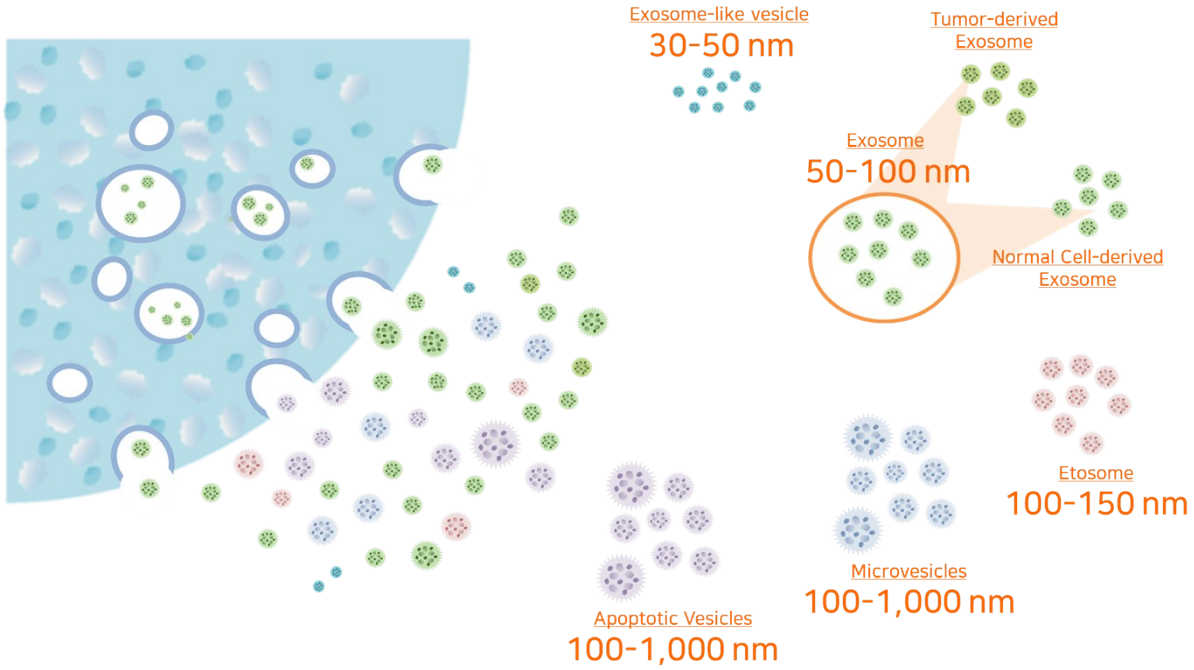

Fig. S8. The classification of extracellular vesicles: exosome, exosome-like vesicles, ectosome, microvesicles, apoptotic vesicles.

S7. Capture Efficiency

Capture efficiency is the fraction of the captured exosomes by an immunofiltration using ExoDIFs. It is one of the most widely used criterion in CTC research; but in this study, we adjusted it to fit the characteristics of exosome research. Due to abundance of circulating exosomes, the calculation was done using particle concentration (per milliliter). In addition, we utilized the concentration of the collected sample to increase accuracy of the evaluation. This means the exosome loss inside device (e.g. trapped, captured-but-not-released, unintentionally damaged, etc.) are not reflected in the results. The classifying of target particle was followed to the determined size range in previous section (**S5. Size Gating for Exosomes and Other Extracellular Vesicles**), and it is calculated as follow.

$$Capture\ Efficiency\ (\%) = [1 - \frac{(Final\ Concentration\ of\ Target\ Vesicles)}{(Initial\ Concentration\ of\ Target\ Vesicles)}$$

Three different model sample with different exosome level was applied to the same ExoDIF device. As we expected, the performance with regard to capture efficiency increased as the exosome level elavated: capture efficiency against Exo-mid and Exo-high sample was 73.35% and 87.08 %, respectively.

Table S1. The analysis based on capture efficiency using model sample including exosome-secreted media (Exo-high), 1:2 diluted exosome-secreted media (Exo-mid), and fresh media containing exosome-depleted FBS (Exo-low)

Device Type		ExoDIFs		
Sample Type		Exo-low	Exo-mid	Exo-high
Capture Efficiency (%)	Avg.	28.83 %	73.35 %	87.08 %
	Stdev.	7.89 %	3.75 %	0.97 %

S8. Background Subtraction Efficiency

The performance of the present device basically depends on the ability of collection exosome-sized vesicles (50 ~ 100 nm). However, proper elimination of non-target vesicles is also important for obtaining highly purified exosome samples through immunofiltration process. In this study, non-target vesicles are also determined based on size of the vesicles. To the best of our knowledge, despite a great diversity of opinion, it has never been reported that exosome-like particles larger than 200 nm. Therefore, we determined the size range of non-target vesicles from 200 nm to 1,000 nm. To evaluate elimination efficiency of these vesicles, we devise a new concept, background subtraction efficiency (BSE), and it is calculated as follow.

$$BSE\ (\%) = [1 - \frac{(Final\ Concentration\ of\ non-target\ Vesicles)}{(Initial\ Concentration\ of\ non-target\ Vesicles)}$$

The following is a comparative table of the present devices regarding to the terms mentioned above. In spite of the fact that it is hard to estimate the initial concentration of non-target vesicles in each sample, we assumed thier concentration showed a reverse tendency as the proportion of exosome increased. However, the results from Exo-mid samples were unexpectedly low (26.83 %); further research regarding the composition of exosome model samples will be required.

Table S2. The analysis based on background subtraction efficiency using model sample including exosome-secreted media (Exo-high), 1:2 diluted exosome-secreted media (Exo-mid), and fresh media containing exosome-depleted FBS (Exo-low)

Device Type		ExoDIFs		
Sample Type		Exo-low	Exo-mid	Exo-high
Background Subtraction Efficiency (%)	Avg.	54.77 %	26.83 %	74.26 %
	Stdev.	3.56 %	1.29 %	3.54 %

S9. Separation Factor

Separation factor is originally a chemistry term referring the efficiency of the separation process: the quotient of the ratio of a certain component to the sum of other components before and after a separation process. We modified this concept for the immunofiltration device based on likeness to chromatography. This factor indicates the possibility of efficient separation; the smaller the factor is, the greater the efficiency of the separation is.

$$Separation\ Factor = \frac{(1 - Background\ Substraction\ Efficiency)}{(Capture\ Efficiency)}$$

The following is a comparative table of the present devices regarding to the terms mentioned above. The factor showed an decreasing tendency according to exosome concentration; in other words, higher efficiency of the separation was achieved against the samples with high exosome concentration.

Table S3. The analysis based on separation factor using model sample including exosome-secreted media (Exo-high), 1:2 diluted exosome-secreted media (Exo-mid), and fresh media containing exosome-depleted FBS (Exo-low)

Device Type		ExoDIFs		
Sample Type		Exo-low	Exo-mid	Exo-high
Separation Factor	Avg.	1.57	1.00	0.30
	Stdev.	0.62	0.04	0.17

S10. Exosome Enrichment Ratio

Exosome enrichment ratio is calculated on the basis of concentration and proportion of exosome-sized vesicles in the sample. Briefly, the ratio between the final concentration and the proportion of the exosome-sized vesicle was divided by the ratio between the initial concentration and the proportion of the exosome-sized vesicle. A ratio of smaller than 1 indicates the purity of the exosome-sized vesicle has diminished during immunofiltration; on the other hand, a ratio of greater than 1 indicates the purity of the exosome-sized vesicle has enhanced at the same time. It is calculated with the changes in concentration and proportion, and it is described as follow:

$$Exosome\ Enrichment\ Ratio = \frac{(Final\ Concen.)/(Final\ Prop.)}{(Initial\ Concen.)/(Initial\ Prop.)}$$

The following is a comparative table of the present devices regarding to the terms mentioned above. The ratio was drastically increased on the results from Exo-high sample. These redults indicated that the exosomes‘ contribution to sample compositon was extensively enhanced after filtration using ExoDIF devices.

Table S4. The analysis based on exosome enrichment ratio using model sample including exosome-secreted media (Exo-high), 1:2 diluted exosome-secreted media (Exo-mid), and fresh media containing exosome-depleted FBS (Exo-low)

Device Type		ExoDIFs		
Sample Type		Exo-low	Exo-mid	Exo-high
Exosome Enrichment Ratio	Avg.	0.29	0.73	3.38
	Stdev.	0.08	0.04	0.36

S11. Particle Size Distribution (PSD)

The particle-size distribution (PSD) is a list of values or a mathematical function that defines the relative amount of particles present according to size. It can offer the information regarding the particle size span width, and D10, D50, and D90 (as known as D-value or three-point specification) is the most widely used values in PSD analysis. Those values indicate the particle diameter at 10 %, 50 %, and 90 % the cumulative distribution. For example, supposing that D50 is 100 nm, it means 50% of the particles in the sample are larger than 100 nm, and 50% smaller than 100 nm. An additional parameters regarding size distribution can be calculated by D10, D50, and D90. For example, span - an indication of the width of the distribution – can be calcluated as follow:

$$Span = \frac{D90 - D10}{D50}$$

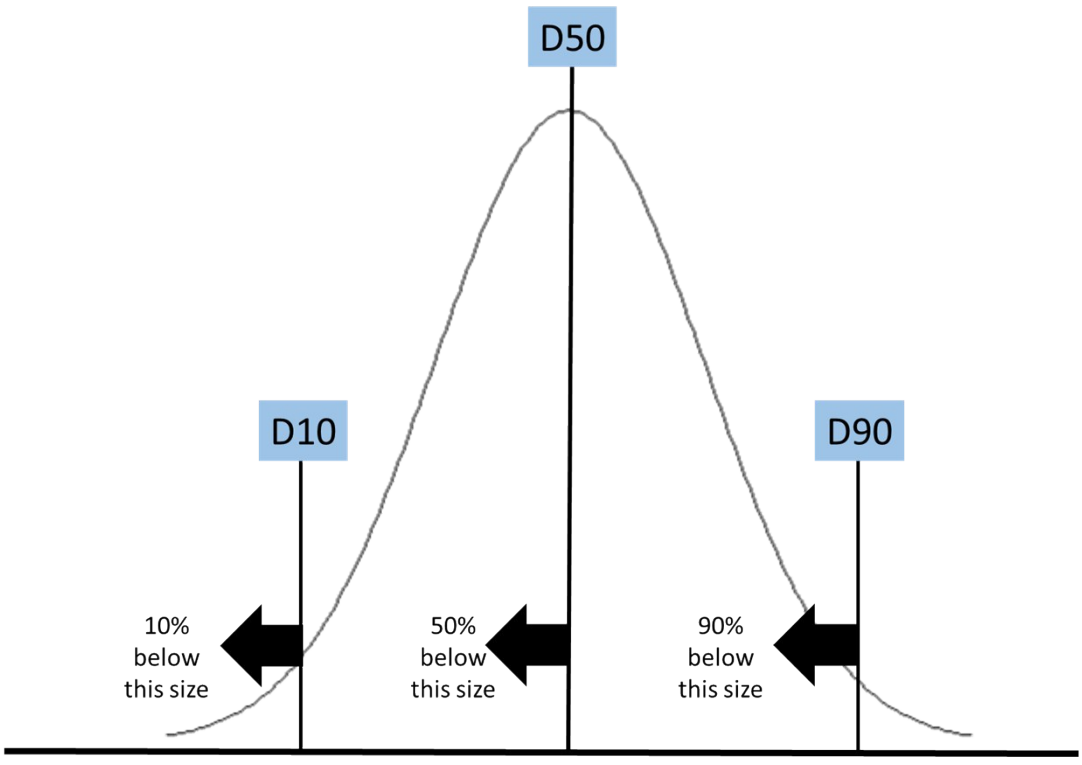

Fig. S9. The definition of particle size distribution D10, D50, and D90.

S12. ExoDIF vs. ExoQuick

ExoQuick kit (System Bioscience, USA) is one of the most widely used method in seoxome separation. When comparing ultracentifugation, which is currently considered as "gold standard," the kit does not require time-consuming and labor-intensive process with multiple steps; however, ExoQuick also have serious issues such as contamination with microvesicles, apoptotic bodies, and polymer components from the kits.[10] Therefore, we verified the feasibility of ExoDIF devices by focusing on sample purity. The present device showed 96.8 % of capture efficiency, and it was comparable to the conventional ExoQuick kit, showing 96.3 % of capture efficiency with the identical sample. However, there was significant difference when comparing the specificity of two methods. The specificity of our device was 94.5 %, while only 86.8 % of particles were in range of size of exosomes when using ExoQuick kit.

Table S5. Comparisons between ExoDIF-based and ExoQuick-based exosome separation using model sample containing 10^6 of exosome-sized particles (Exo-6).

		Exo-6			
		ExoDIF		ExoQuick	
		Before immunofiltration	After immunofiltration	Before separation	After separation
Particle Size Distribution (PSD)	Mean (nm)	76.0 ± 6.2	198.0 ± 24.1	76.0 ± 6.2	246.5 ± 3.5
	Mode (nm)	22.0 ± 3.4	157.5 ± 9.2	22.0 ± 3.4	157.0 ± 52.3
	D10 (nm)	20.0 ± 1.8	121.0 ± 8.5	20.0 ± 1.8	105.0 ± 5.7
	D50 (nm)	53.0 ± 6.9	182.5 ± 17.7	53.0 ± 6.9	189.5 ± 33.2
	D90 (nm)	170.0 ± 10.2	325.0 ± 11.3	170.0 ± 10.2	571.0 ± 207.9
	Span	2.83	1.12	2.83	2.46
Capture Efficiency		96.77 ± 1.42 %		96.27 ± 0.47 %	
Background Subtraction Efficiency		84.49 ± 0.39 %		89.22 ± 0.10 %	
Separation Factor		0.16 ± 0.01		0.11 ± 0.02	
Exosome Enrichment Ratio		6.24 ± 0.15		8.93 ± 0.14	
Specificity		94.45 ± 2.31 %		86.74 ± 1.77 %	

S13. Capturing Appearance of the Exosomes

In order to investiate capturing appearance of the exosomes on the patterns of ExoDIF devices, the FE-SEM images were obtained with the higher magnification. **Fig. S7** shows the pattern of the bottom layer (left) and the enhanced image of the upper surface (right). These images were taken from the ExoDIF devices after processing of exosomes-containing sample. There were abundant exosome-sized particles in range of the size of exosome and they were also evenly distributed through out the device. Definately, these small lumps were not found inside bare ExoDIF device or after processing of the noraml buffer with ExoDIF device. The results indicate that the exosome-sized particles are capable to be captured by processing through the present device.

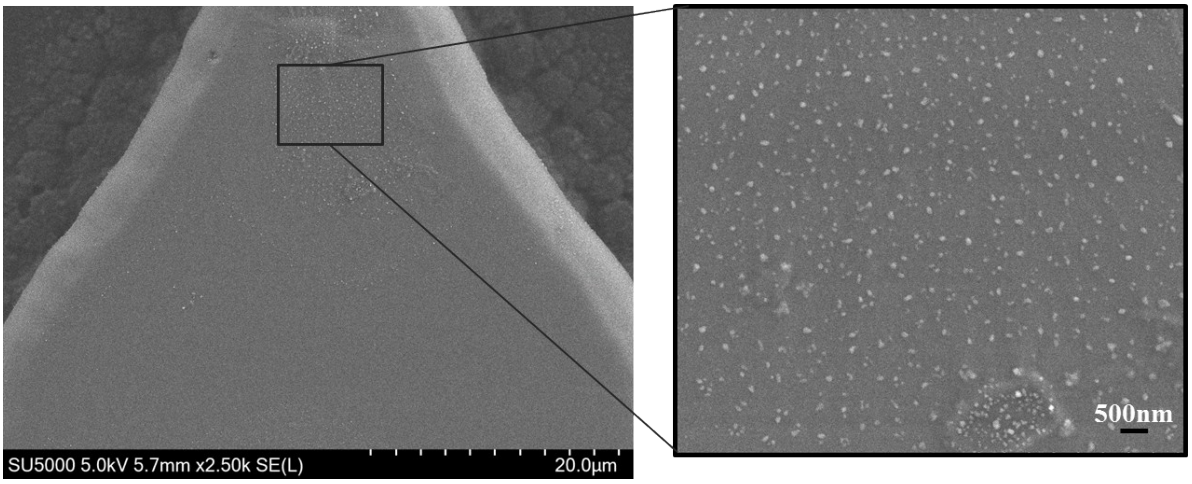

Fig. S10. The FE-SEM image of the MCF-7 human breast cancer cell-secreted exosomes captured on the bottom layer of the ExoDIF with the enlarged view of individual exosomes. The images were magnified by a factor of 500 and 10,000 with an acceleration voltage of 10.0 kV.

S14. Exosome Stability Against Dithiothreitol

A reducing agent, dithiothreitol (DTT) have been applied to several urinary exosome studies for identification and proteomic profiling to eliminate the interference induced by background proteins, especially Tamm-Horsfall (THP) protein.[11-13] In the afformentioned works, most researchers determined the appropriate concentration of DTT solution is approximately 200 mg/ml. In some cases, the exosome containing samples are exposed to the solution during multi-step centrifugation. It is much higher concentration and longer incubation compared to the suggested condition in the protein research (1~100 mM; less than 30 mins)[14, 15] or the cytotoxicity research (25~500 uM; less than 30 mins).[16, 17] This implies that exosomes are not easily damaged by DTT unlike cells or glycoproteins; thus, we assume that a certain level of exposure does not affect to the proteomic profiling of exosomes. According to our experience, there were no difference in the number of exosome-sized particles between DTT-treated sample and non-treated samples (data not shown). Definitely, we have also thoroughly considered the possibility that blood serum exosome might not have the identical characteristics with urinary exosome; the sufficient evidence that two types of exosome have much different level of stability against chemical agents are not fully validated yet.[18]

S15. Patients information

Table S6. Information of samples involved in the present studies including FE-SEM analysis, nanoparticle tracking analysis and on-chip EpCAM expression.

	ID	Sex	Age	Cancer Type	Location	Stage	Classification	Differentiation	Metastasis	Recurrence	Note
Cancer Patient	*CP1*	M	46	Colon	sigmoid	IV	adenocarcinoma	M/D	liver, peritoneal seeding	-	-
	CP2	F	70	Colon	rectal	III	adenocarcinoma	M/D	lung	Yes	-
	CP3	M	59	Colon	rectal	III	adenocarcinoma	P/D	LN	Yes	-
	CP4	M	60	Colon	sigmoid	IV	adenocarcinoma	M/D	LN, bone	-	-
	CP5	F	52	Breast	Breast	II	TNBC	-	No metastasis	-	ER+/ HER+
	CP6	F	53	Breast	Breast	III	Luminal B	-	No metastasis	-	-
Healthy Donors	*HD1*	F	25	-							-
	HD2	M	25	-							-
	HD3	M	27	-							-
	HD4	M	26	-							-
	HD5	M	21	-							-

Reference

1. J. Bu, Y. T. Kang, Y. J. Kim, Y. H. Cho, H. J. Chang, H. Kim, B. I. Moon and H. G. Kim, *Lab Chip*, 2016, **16**, 4759-4769.
2. C. Thery, L. Zitvogel and S. Amigorena, *Nat Rev Immunol*, 2002, **2**, 569-579.
3. Q. Zhou, A. Rahimian, K. Son, D. S. Shin, T. Patel and A. Revzin, *Methods*, 2016, **97**, 88-93.
4. K. Denzer, M. J. Kleijmeer, H. F. G. Heijnen, W. Stoorvogel and H. J. Geuze, *Journal of Cell Science*, 2000, **113**, 3365-3374.
5. A. A. Sina, R. Vaidyanathan, S. Dey, L. G. Carrascosa, M. J. Shiddiky and M. Trau, *Sci Rep*, 2016, **6**, 30460.
6. W. Oosthuyzen, N. E. Sime, J. R. Ivy, E. J. Turtle, J. M. Street, J. Pound, L. E. Bath, D. J. Webb, C. D. Gregory, M. A. Bailey and J. W. Dear, *J Physiol*, 2013, **591**, 5833-5842.
7. F. Hawari, F. Rouhani, X. Cui, Z. Yu, C. Buckley, M. Kaler and S. Levine, *PNAS*, 2004, **101**, 1297-1302.
8. D. D. Poutsiaka, E. W. Schroder, D. D. Taylor, E. M. Levy and P. H. Black, *The Journal of Immunology*, 1985, **134**, 138-144.
9. C. Hess, S. Sadallah, Andreas Hefti, e. Landmann and J.-A. Schifferli, *The Journal of Immunology*, 1999, **163**, 4564-4573.
10. A. Safdar, A. Saleem and M. A. Tarnopolsky, *Nat Rev Endocrinol*, 2016, **12**, 504-517.
11. P. Fernandez-Llama, S. Khositseth, P. A. Gonzales, R. A. Star, T. Pisitkun and M. A. Knepper, *Kidney Int*, 2010, **77**, 736-742.
12. P. A. Gonzales, T. Pisitkun, J. D. Hoffert, D. Tchapyjnikov, R. A. Star, R. Kleta, N. S. Wang and M. A. Knepper, *J Am Soc Nephrol*, 2009, **20**, 363-379.
13. T. Pisitkun, R.-T. Shen and K. M.A., *PNAS*, 2004, **101**, 13368-13373.
14. C. S. Thaxton, H. D. Hill, D. G. Georganopoulou, S. I. Stoeva and M. C.A., *Analytical Chmemistry*, 2005, **77**, 8174-8178.
15. W. Lee, B.-K. Oh, Y. Min Bae, S.-H. Paek, W. Hong Lee and J.-W. Choi, *Biosensors and Bioelectronics*, 2003, **19**, 185-192.
16. M. E. Solovieva, V. V. Solovyev, A. A. Kudryavtsev, Y. A. Trizna and V. S. Akatov, *Free Radic Biol Med*, 2008, **44**, 1846-1856.
17. M. H. Aghdai, A. Jamshidzadeh, M. Nematizadeh, M. Behzadiannia, H. Niknahad, Z. Amirghofran, E. Esfandiari and N. Azarpira, *Hepat Mon*, 2013, **13**, e7824.
18. M. Li, E. Zeringer, T. Barta, J. Schageman, A. Cheng and A. V. Vlassov, *Philos Trans R Soc Lond B Biol Sci*, 2014, **369**.